Search for NMSSM Higgs $h \to aa \to \mu\mu\mu\mu$

(Dated: April 6, 2009)

We present a study ...

PACS numbers: 13.38.Dg 13.38.Qk

I. INTRODUCTION

Tension between the electroweak data fits preferance for light higgs and limits from direct searches can be resolved by an elegant solution handed by the NMSSM. A possible solution could be that there is a new mode for higgs decay $h \to aa$, where a is a pseudoscalar higgs field, thus diminishing the branching ratios for conventional modes used in direct higgs searches and largely softening direct higgs mass limits from LEP. While 'naturalness' and 'fine tuning' arguments have lead to somewhat extensive studies of the region of masses of a above $\tau\tau$ and $b\bar{b}$ threshold, the results require a substantial integrated luminosity and are technically very challenging analysis.

At the same time, the region of lower masses (below $2m_\tau$) has not been studied. We propose here an analysis targeting the range of m_a below the $\tau\tau$ threshold by exploring the decay $h \to aa\mu\mu\mu\mu$. Unlike searches with taus, the two muon mass gives a direct estimate of m_a providing a substantially better constrained system. Further, this channel is essentially free of backgrounds and therefore one can use direct gluon fusion production instead of smaller vector boson fusion process that has to be used in order to suppress large QCD backgrounds.

Current constraints in this region come from XXX and are fairly weak - need SASHA's help here.

We show that the analysis in the four muon mode has excellent sensitivity for higgs and can be performed with just a handful of first CMS data and requires very little in terms of detector performance except reasonably robust tracking for muons and well functioning muon system. To make this a realistic analysis, we use parameters of the CMS experiment in designing selections and estimating background contributions.

II. NMSSM PARAMETER SPACE

The allowed NMSSM parameter space permits at least two phenomenologically-distinct Higgs systems, one in which a 120 GeV scalar Higgs decays primarily into conventional WW^*, $b\bar{b}$, and $\tau^+\tau^-$ modes, and another with a light, hidden Higgs that decays almost exclusively into aa. The latter has only been excluded up to 86 GeV by specialized searches at LEP (upper limit due to $e^+e^- \to hZ$ kinematics) [23, 24], leaving the 86–120 GeV region unexplored (Fig 1).

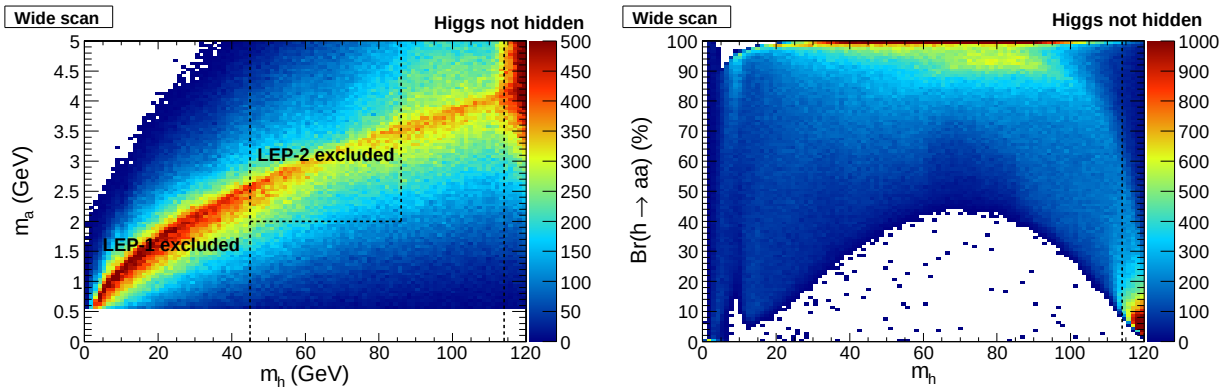

FIG. 1: Left: regions of m_a vs. m_h excluded by LEP searches, right: the strong correlation between m_h and $B_{h\to aa}$. The above scan is subject to experimental constraints (other than the two specialized LEP searches for $h \to aa$) which require a conventionally-decaying Higgs to have $m_h > 114$ GeV.

We used the NMSSMTools package [25–27] to scan the NMSSM parameter space and to identify the region with $B_{h\to aa} \gg B_{h\to WW^*,\, b\bar{b},\, \tau^+\tau^-}$. Scans are uniform in each parameter listed in Table I, subject to phenomenological and experimental constraints except for the specialized LEP $h \to aa$ searches. Two scans were performed, labeled "wide" and "narrow," where the narrow scan focuses more exclusively on the hidden Higgs region. The λ and A_κ parameters are restricted even in the wide scan to yield small m_a values, important for large $B_{a\to\mu\mu}$. A particularly important

parameter for distinguishing between conventional Higgs decays and hidden decays is the ratio of κ over λ, so we perform uniform scans in this ratio, rather than κ alone. Fig 3 shows how each parameter is related to $B_{h\to aa}$.

TABLE I: Ranges for NMSSM parameter scans. The narrow scan focuses on the region with high $B_{h\to aa}$.

Wide scan	Narrow scan
$0 < \kappa/\lambda < 0.8$	$0 < \kappa/\lambda < 0.5$
$0 < \lambda < 0.1$	*same*
$-0.1 < A_\kappa < 0$ GeV	*same*
$0 < A_\lambda < 4$ TeV	$1 < A_\lambda < 3$ TeV
$100 < \mu < 200$ GeV	$100 < \mu < 150$ GeV
$10 < \tan\beta < 60$	$10 < \tan\beta < 33$

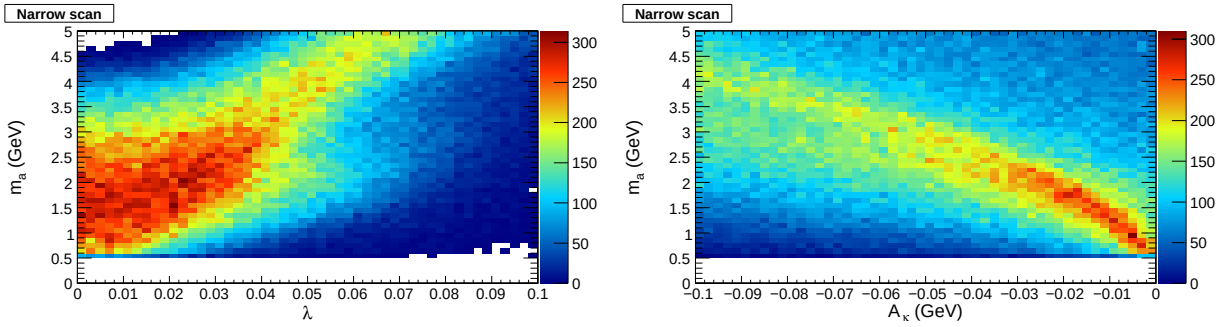

FIG. 2: Both λ and A_κ must be close to zero for m_a to be below the $2\,m_\tau$ threshold.

To determine the sensitivity of our 4-muon search channel, we also need to know the branching fraction of $a\to\mu\mu$. In the mass range of interest (below the $a\to\tau^+\tau^-$ threshold), the main competing channels are $a\to gg$ and $a\to s\bar{s}$. We again use NMSSMTools to calculate these (with $m_s = 95$ MeV and no cut on m_a), which are nearly a function of m_a only. The final branching fractions are presented in Fig 4.

A. Production Cross Section $pp\to h + X$

Due to relatively low expected backgrounds in the case of the four muon channel, one should go after the dominant production modes of higgs boson. We include $gg\to h$ and $bb\to h$. The higgs production cross-section is calculated in the framework of NMSSM for typical sets of parameters using XXX and YYY. Figure 2 shows the predicted cross-section for several typical choices of parameters and also a comparison with the Standard Model higgs production cross-section. **Need Sasha to write this one!!!**

III. ANALYSIS

The main characteristics of the anaysis are two back-to-back pairs of spatially close muons. Each of the di-muon pairs should have invariant mass consistent with m_a and the four muon invariant mass should give a bump corresponding to the higgs mass. We use these facts in designing an analysis with a reasonably high acceptance and very low backgrounds suitable for early LHC running.

A. Signal Simulation

We used Pythia to generate signal events (should we give settings?). We generated samples with $m_h \times m_a = (70, 80, 90, 100, 110, 120\ GeV/c^2) \times (1, 1.5, 2, 2.5, 3\ GeV/c^2)$. We used XXX to emulate detector response (major

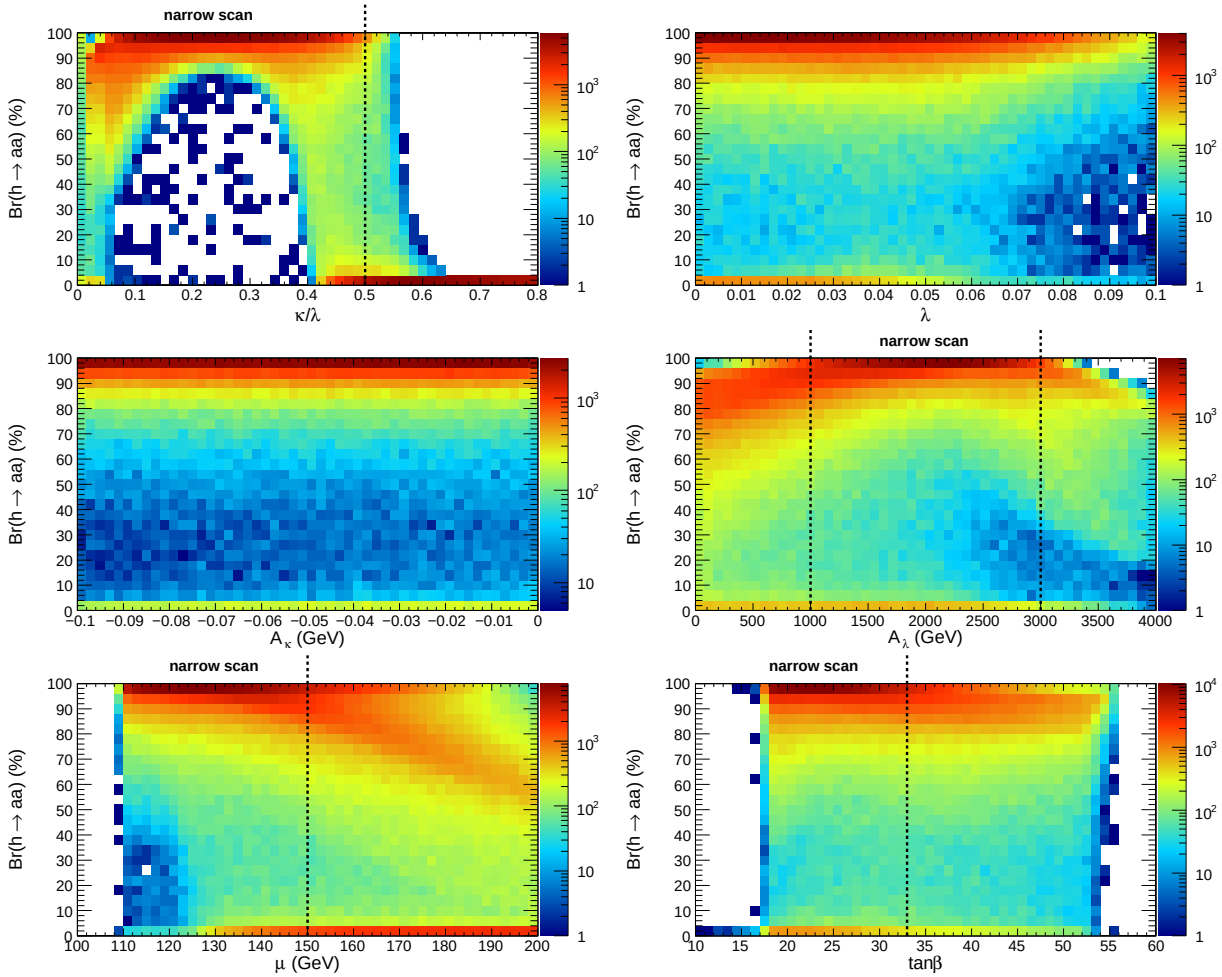

FIG. 3: $B_{h\to aa}$ as a function of each of the NMSSM parameters with dashed lines indicating the "narrow scan" cuts (Table I). All narrow scan cuts are applied except for the one shown. Note the logarithmic color scale used to highlight the difference between $B_{h\to aa} \approx 0\%$ and $\approx 100\%$.

parameters are muon momentum resolution, low threshold on muons to reach the muon system, acceptance and average reconstruction efficiencies that were taken from CMS TDR).

Figure 3 and 4 show invariant masses of the muon pairs (we force correct assignment of pairs using generator information) and of the 4 muon system.

B. Event Reconstruction

The analysis starts by requiring at least four muon candidates with $p_T > 5$ GeV/$c$in the fiducial volume of the detector. At least one of the four muons has to have $p_T > 20$ GeV/$c$to satisfy likely trigger requirements. Each event must have at least two muon candidates of positive and negative charge. In events satisfying these critiria, we define quadruplets of candidates consisting of two positive and two negatively charged muon candidates. Note that at this point there could be more than one quadruplet per event, e.g. if there are five muons in the event.

At the next step, inside each quadruplet, we sort out the four muon candidates into two pairs (pairs will later beassociated to one of the two axial bosons a). We perform this assignment by requiring that in each pair there must be two muon candidates of opposite charge and minimizing the $MIN_{(i,j,k,l)}(\Delta R(\mu_i,\mu_j)^2 + \Delta R(\mu_k,\mu_l)^2)$ to determine the most likely assignment of four muons into two pairs $(i,j)\bigoplus(k,l)$. **Figure 5 shows the distribution for this value showing high efficiency of this algorithm for the range of** (m_h, m_a) **values of interest to this analysis.** At his point muon candidates are assigned into pairs and invariant mass of each of the pair (we denote the pair masses as $m_{12} and m_{34}$) is calculated as well as invariant mass of all four muons, we denote it as m_{1234} or M. Fig. **??** shows

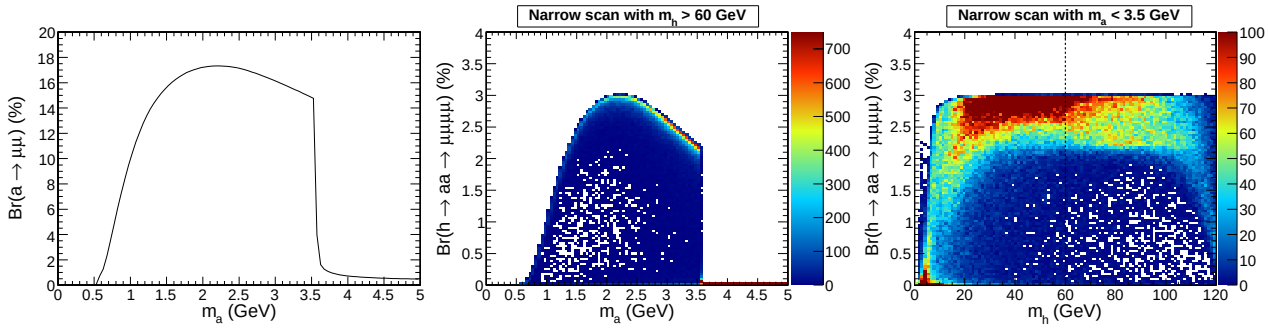

FIG. 4: Branching fractions of $a \to \mu\mu$ and full $h \to aa \to \mu\mu\mu\mu$ chain as a function of m_a and m_h.

TABLE II: Acceptances for various points in m_h-m_a space.

m_h, m_a (GeV)	0.5	1.0	2.0	3.0	4.0
80	0.3052 ± 0.0046	0.2656 ± 0.0044	0.2420 ± 0.0043	0.2389 ± 0.0043	0.2324 ± 0.0043
100	0.3915 ± 0.0049	0.3245 ± 0.0047	0.2906 ± 0.0045	0.2862 ± 0.0045	0.2819 ± 0.0045
120	0.4587 ± 0.0050	0.3785 ± 0.0049	0.3405 ± 0.0047	0.3226 ± 0.0047	0.3103 ± 0.0046

the distribution of invariant masses of such pairs for signal events with $(m_h, m_a) = (90, 0.5)$ GeV/c^2(solid line) and $(m_h, m_a) = (90, 2.5)$ GeV/c^2that passed all previous selections. Figure **??** shows the distribution of the four muon invariant mass, M, for signal events generated with $(m_h, m_a) = (70, 1.5)$ (solid line) and $(120, 1.5)$ GeV/c^2(dashed line).

We consider adding isolation requirements to muons to decrease the fraction of the muons originating from jets. That should go along the lines of what we discussed earlier (isolation of the pair, not individual muons).

The kinematics of signal events and the specific interest of this analysis in the region of $0.5 < m_a < 3.6$, $m_h > 60$ GeV/c^2, one could reasonably apply additional selections on m_{12}, m_{34}, m_{1234} and $|m_{12} - m_{34}|$ (to enforce the requirement that the two pair masses are consistent with each other). We choose to keep all remaining events and instead develop a fitting procedure that works in a 3D space $(m_{12}, m_{34}, m_{1234})$ that is aware of special kinematical properties of signal events (they will appear as a bump in one specific small region in this 3D space). Our approach allows preserving all available acceptance and maximize statistical power of the analysis. It is also convenient from experimental point of view as the backgrounds will be distributed in some smooth fashion over the 3D space allowing fitting the 3D distribution to estimate backgrounds directly from the data.

Acceptance for these cuts is shown in Table II. Note Figures 9 and 10 show acceptance as a function of m_h for several fixed m_a and as a function of m_a for several choices of m_h values. - we should recalculate acceptances corresponding to this point, currently they are quoted for after the next series of 'illustrational' cuts.

However, to give reader a better idea of the signal and background rates in the region consistent with the signal kinematics and the target region of this analysis, we also quote overall acceptance (and later background efficiencies and rates) for the following cuts as if they were applied after the main cuts above: both pair reconstructed mass values, m_{12} and m_{34}, should be less than 4 GeV/c^2; the invariant mass of the four muons m_{1234} >60 GeV/c^2; and $|m_{12} - m_{34}| < X$ GeV/c^2.

we need to add plots for pair mass (m_{12}, m_{34}, m_{1234}, $m_{12} - m_{34}$.

Table II shows acceptances for different points in m_h-m_a space.

C. Background Estimation

1. *QCD backgrounds*

Requirement of four muons in the event selection drastically reduces contributions of background processes. The largest contribution comes from rare QCD events where four real muons are produced in heavy flavor decays of b and

c mesons. This background can be substantially reduced by the requirement of at least one muon with $p_T > 20$ GeV/c and can be estimated using Pythia Monte Carlo. Another QCD background comes from events with two or three real muons from heavy flavor decays and the remaining candidates come from misidentification dominated by K/π decays in flight. This background can be estimated using the same Pythia sample by selecting events with two or three real muons and a charged pion or kaon satisfying p_T and η requirements used in this analysis for muons and weighing such combinations with the probability to decay into a muon before reaching radius of $\simeq$2 meters. We find that the level of backgrounds due to misidentifications is comparable to the rate of the backgrounds associated with real muons from heavy flavor decays. However, both of these contributions are further suprpessed by the requirement of the four muon invariant mass to be above 60 GeV and a requirement that pairs of such muons have low invariant mass. While the fraction of remaining events at this point is still not negligible, the probability that muon candidates in background events can be arranged in pairs of similar invariant masses is very small making QCD contributions nearly negligible. One can essentially completely eliminate these backgrounds by applying loose track isolation requirement on each of the pairs.

We used Pythia Monte Carlo to simulate four muon QCD backgrounds using 2→2 QCD production where we required at least one muon (either real from e.g. b or c quark decays or from pion and kaon decays in flight) with transverse momentum above 20 GeV/c (to be consistent with the definition of non-isolated inclusive muon trigger at CMS). In addition, we generated a large sample of J/ψ events. Other SM backgrounds (ZZ*, top) were foudn to be small in the mass region of interest. Figure 7 and 8 show the same distributions as in Figures 3 and 4, but for the signal + SM backgrounds overlayed. Note that these plots are not reflective of the true significance of signal over background because these plots do not take into account that the two pair masses must be consistent with each other and simultaneously form a narrow peak in the four muon mass.

2. J/ψ

We also studied direct J/ψ production process that can produce a pair of muons with mass in the range of interest of this analysis and another pair of muons can come from decays in flight. We used Pythia MC and a weighing technique similar to the QCD case and find that this background is completely negligible.

3. Electroweak four lepton backgrounds

We use CompHEP to generate a large sample of events with four muons in final state coming from electroweak processes. The cross-section of this process is 0.5 pb (**Sasha, is this correct? Kind of sounds very small!!!**) and after a cut on the first muon $p_T > 20$ GeV/c, the large chunk of remaining events are $Z\gamma^*$ type events. Very few of these events have muons that can be arranged into pairs with low invariant mass, and the fraction of events with similar masses of the pairs is completely negligible.

4. Summary

While the number of events going into the final fit is not small, the fitting procedure described in the next section is effectively reducing the region of interest to events that have similar invariant masses of the two pais of muons, which leaves us in essentially zero background situation. Tables **??** show efficiency of passing sequential cuts for each type of backgrouns as well as the number of expected background events after each cut in a dataset corresponding to 100 pb^{-1}of LHC data.

IV. STATISTICAL ANALYSIS OF THE DATA

To maximize sensitivity and emulate real data analysis techniques, we define a likelihood function in the 3D space ($m_{pair\ 1},\ m_{pair\ 2}, M$), where M is the four muon invariant mass. The likelihood is defined as follows:

$$\mathcal{L}(m_h, m_a, \sigma(pp{\rightarrow}h)) = \prod_i \mathcal{P}(\sigma(pp{\rightarrow}h) L B_{h\rightarrow aa} B^2_{a\rightarrow\mu\mu} L\alpha(m_h, m_a) S_i(m_a, m_h) + LB_i, N_i^D) \quad (1)$$

where i runs over bins in 3D space of (m_{12}, m_{34}, m_{1234}), m_h is light higgs mass, m_a is axial mass, $\mathcal{P}(\nu, N)$ is Poisson probability for observing N events when the true rate is ν, L is luminosity, α is acceptance of the signal events, S_i is the fraction of reconstructed signal events in bin i, B_i is the rate of background events in bin i per unit of luminosity.

TABLE III: Background cuts efficiency for generator level

Cuts	4 leptons	$\mu + x$	J/Ψ
1st eta<2.4	0.7994 ± 0.0040	0.95638 ± 0.00073	0.0088 ± 0.0022
2nd eta<2.4	0.8295 ± 0.0042	0.99992 ± 0.00003	$1.00^{+0.00}_{-0.06}$
3rd eta<2.4	0.8541 ± 0.0044	0.99584 ± 0.00024	0.75 ± 0.11
4th eta<2.4	0.7066 ± 0.0061	0.96407 ± 0.00068	0.75 ± 0.13
1st pt>5	0.9805 ± 0.0022	$1.00000^{+0}_{-0.00001}$	$1.0^{+0.0}_{-0.1}$
2nd pt>5	0.9405 ± 0.0038	0.8676 ± 0.0013	$1.0^{+0.0}_{-0.1}$
3rd pt>5	0.7893 ± 0.0068	0.0445 ± 0.0008	0.3333 ± 0.1571
4th pt>5	0.4390 ± 0.0093	0.0284 ± 0.0032	$0.00^{+0.27}_{-0.00}$
1st pt>20	0.9524 ± 0.0060	0.9873 ± 0.0126	0
analysis acceptance	0.1218 ± 0.0033	0.00099 ± 0.00011	0
pair masses<4	0.0025 ± 0.0014	0.3333 ± 0.0533	0
inv. mass>60	0.6667 ± 0.3333	0.4231 ± 0.0969	0
$\lvert m_{12} - m_{34} \rvert$ <X GeV	$X.XXXX \pm X.XXXX$	$X.XXXX \pm X.XXXX$	0
full efficiency	0.000203 ± 0.000143	0.00014 ± 0.00004	0

TABLE IV: Background cuts efficiency for reco level

Cuts	4 leptons	$\mu + x$	J/Ψ
1st pt>5	0.7455 ± 0.0044	$1.00000^{+0}_{-0.00001}$	$1.0000^{+0}_{-0.0006}$
2nd pt>5	0.7012 ± 0.0053	$1.00000^{+0}_{-0.00001}$	$1.0000^{+0}_{-0.0006}$
3rd pt>5	0.6066 ± 0.0068	0.04349 ± 0.0007	0.3333 ± 0.0013
4th pt>5	0.3300 ± 0.0084	0.0402 ± 0.0034	$0.00^{+0.15}_{-0.00}$
1st pt>20	0.9573 ± 0.0063	$1.000^{+0}_{-0.007}$	0
analysis acceptance	0.1002 ± 0.0030	0.0017 ± 0.0002	0
pair masses<4	0.0041 ± 0.0020	0.3358 ± 0.0403	0
inv. mass>60	0.50 ± 0.25	0.4348 ± 0.0731	0
$\lvert m_{12} - m_{34} \rvert$ <X GeV	$X.XXXX \pm X.XXXX$	$X.XXXX \pm X.XXXX$	0
full efficiency	0.00020 ± 0.00014	0.00025 ± 0.00006	0

We have studied QCD background events in the Monte Carlo and found that their distribution in the (m_{12}, m_{34}, M) space can be parameterized the following function:

$$B(m_{12}, m_{34}, m_{1234}) = f(m_1 2) \times f(m_3 4) \times g(m_{1234}). \quad (2)$$

Parameters of the function are shown in Table **??** and were obtained by fitting the distribution of invariant masses of pairs. Note that in the analysis we randomly assign pairs of muons as 'first' or 'second' pair to ensure they have the same distribution. We verified that background events found in MC are well described by this function by running pseudoexperiments using paramaterized distribution and verifying that the p-value for the outcome similar to what is observed in MC is high.

A. Exclusion Levels if No Excess Observed

Thus defined, the likelihood function is sufficient to calculate the 95% C.L. exclusion region in (m_a, m_h) parameter space. We run pseudoexperiments with background only (no signal) to calculate the 95% C.L. on the product $\sigma(pp{\to}h)B_{h\to aa}B^2_{a\to\mu\mu}\,\alpha$, which is 0.0293 pb at $L = 100$ pb^{-1}, approximately 3 events. This result is independent of m_h and m_a because the effective signal region tested by the fitter is background free.

Since $B_{a\to\mu\mu}$ is nearly a function of m_a only, it can be factored out, and the corresponding upper limit on $\sigma(pp{\to}h)B_{h\to aa}\alpha$ is presented in Table VII. The upper limit on $\sigma(pp{\to}h)B_{h\to aa}$ is shown as a function of m_h and m_a in Table VIII by factoring out α as well. Keep in mind that $B_{h\to aa}$ is close to 100% in much of our preferred region of NMSSM parameter space.

TABLE V: Number of events after each selection cut on generator level

Cuts	4 leptons	Incl. muon	JPsi
Initial number	48.21 ± 0.49	152878.11 ± 546.06	120.91 ± 2.84
1st eta<2.4	38.54 ± 0.43	146209.61 ± 534.01	1.0652 ± 0.2663
2nd eta<2.4	31.97 ± 0.40	146197.91 ± 533.99	1.0652 ± 0.2663
3rd eta<2.4	27.30 ± 0.37	145589.38 ± 532.88	0.7989 ± 0.2306
4th eta<2.4	19.29 ± 0.31	140358.34 ± 523.22	0.5992 ± 0.1997
1st pt>5	18.92 ± 0.30	140358.34 ± 523.22	0.5992 ± 0.1997
2nd pt>5	17.79 ± 0.30	121774.70 ± 487.35	0.5992 ± 0.1997
3rd pt>5	14.04 ± 0.26	5424.13 ± 102.86	0.1997 ± 0.1153
4th pt>5	6.17 ± 0.17	154.08 ± 17.34	0
1st pt>20	5.87 ± 0.17	152.13 ± 17.23	0
pair masses<4	0.0147 ± 0.0085	50.71 ± 9.95	0
inv. mass>60	0.0098 ± 0.0069	21.45 ± 6.47	0
$\lvert m_{12} - m_{34}\rvert$ <X GeV	$X.XXXX \pm X.XXXX$	$X.XXXX \pm X.XXXX$	0

TABLE VI: Number of events after each selection cut on reco level

Cuts	4 leptons	Incl. muon	JPsi
Initial number	48.21 ± 0.49	152878.11 ± 546.06	120.91 ± 2.84
1st pt>5	35.94 ± 0.42	152878.11 ± 546.06	120.91 ± 2.84
2nd pt>5	21.20 ± 0.35	152878.11 ± 546.06	0.3995 ± 0.1631
3rd pt>5	15.29 ± 0.27	6648.99 ± 113.88	0
4th pt>5	5.04 ± 0.16	267.21 ± 22.83	0
1st pt>20	4.83 ± 0.15	267.21 ± 22.83	0
pair masses<4	0.0049 ± 0.0098	89.72 ± 13.23	0
inv. mass>60	0.0098 ± 0.0069	39.01 ± 8.72	0
$\lvert m_{12} - m_{34}\rvert$ <X GeV	$X.XXXX \pm X.XXXX$	$X.XXXX \pm X.XXXX$	0

B. Discovery Levels if Excess Observed

Figure **??** shows results of a pseudoexperiment in which pseudodata was a combination of background events and signal with $\sigma(pp\to H)$=10 pb^{-1}, $B(H\to aa\to\mu\mu\mu\mu)$=0.04, m_a = 3 GeV, m_h = 100 GeV. The plot shows likelihood function $\mathcal{L}(m_h, m_a, \sigma(pp\to h))$ vs $\sigma(pp\to h)$ for m_h and m_a set to the true values. It is clear that significance of such signal is very large.

However, in real experiment, one does not look at fixed values of m_a and m_h. Instead, one scans likelihood function searching for an overall maximum in the $m_a, m_h, \sigma(pp\to H)$ space. Probability of oberving an excess of certain significance due to background fluctuation anywhere in the range is much larger than observing it in any a

TABLE VII: 95% C.L. on $\sigma(pp\to h)B_{h\to aa}\,\alpha$ at $L = 100$ pb^{-1} as a function of m_a, from Fig 4.

m_a (GeV)	$B_{a\to\mu\mu}$ (%)	$\sigma(pp\to h)B_{h\to aa}\,\alpha$ (pb)
0.5	0	∞
0.75	4.2	16.5
1.0	10.0	2.9
1.5	15.7	1.2
2.0	17.2	1.0
2.5	17.1	1.0
3.0	16.1	1.1
3.5	14.8	1.3
3.75	1.02	282
4.0	0.73	557
5.0	0.49	1220

TABLE VIII: 95% C.L. on $\sigma(pp\rightarrow h)B_{h\rightarrow aa}$ (pb) at $L = 100$ pb^{-1}, from Fig 4 and Table II.

m_h, m_a (GeV)	0.5	1.0	2.0	3.0	4.0
80	∞	10.9	4.1	4.6	2400
100	∞	8.9	3.4	3.8	2000
120	∞	7.7	2.9	3.4	1800

priori chosen point in m_a, m_h, therefore significance has to be corrected to account for the fact that we essentially run many searches at the same time.

Rather then attempting to obtain 'trial factor' analytically, the practical solution is to calculate the p-value, which is the probability of observing a fake signal from background fluctuation as significant as the one seen in data anywhere in the range analyzed in the measurement.

For simplicity we choose to scan data using a 2D grid in $(m_h \times m_a) = (60 - 200) \times (0.1, 4.0)$ with a step of 3 GeV in m_h direction and 0.1 GeV in m_a direction. These values are chosen to be small enough to not miss a likely signal.

To obtain smooth lines between the points in which signal samples were generated, we interpolated $S_i(m_h, m_a) = (S_i(m_h^j, m_a^j) + S_i(m_h^j + 1, m_a^j + 1))/2$, where j refers to nearest generated sample with lower masses, $j + 1$ to the nearest sample with hhigher masses.

V. RESULTS

TO BE WRITTEN

Acknowledgments

We thank XXX and YYY

[1] C. Albajar *et al.* (UA1 Collaboration), Phys. Lett. B **253**, 503 (1991); J. Alitti *et al.* (UA2 Collaboration), Phys. Lett. B **276**, 365 (1992).
[2] The LEP Collaborations: ALEPH, DELPHI, L3 and OPAL, the LEP Electroweak Working Group and the SLD Electroweak and Heavy Flavor Working Group (2004), hep-ex/0412015.
[3] T. Affolder *et al.* (CDF Collaboration), Phys. Rev. Lett. **84**, 845 (2000); F. Abe *et al.* (CDF Collaboration), Phys. Rev. D **59**, 052002 (1999); S. Abachi *et al.* (DØ Collaboration), Phys. Rev. Lett. **75**, 1456 (1995); B. Abbot *et al.* (DØ Collaboration), Phys. Rev. D **60**, 053003 (1999).
[4] D. Acosta *et al.* (CDF Collaboration), Phys. Rev. Lett. **94**, 091803 (2005); A. Abulencia *et al.* (CDF Collaboration), FERMILAB-PUB-05-360 (2005), Submitted to Phys. Rev. D.
[5] V.M. Abazov *et al.* (DØ Collaboration), Phys. Rev. D **71**, 072004 (2005).
[6] M. Carena *et al.* , hep-ph/0010338; M. Carena *et al.* , Eur. Phys. J. C **26**, 601 (2003); S. Abel *et al.* , hep-ph/0003154.
[7] S. Belyaev, T. Han, and R. Rosenfeld, JHEP **0307**, 021 (2003).
[8] A. Dedes *et al.* , hep-ph/0207026.
[9] A. Abulencia *et al.* (CDF Collaboration), Phys. Rev. Lett. **96**, 011802 (2006); D. Acosta *et al.* (CDF Collaboration), Phys. Rev. Lett. **95**, 131801 (2005) .
[10] D. Acosta *et al.* (CDF Collaboration), Phys. Rev. D **72**, 072004 (2005).
[11] D. Acosta *et al.* (CDF Collaboration), Phys. Rev. D **71**, 032001 (2005).
[12] S. Baroiant *et al.* , Nucl. Instrum. Methods A **518**, 609 (2004).
[13] S. Klimenko, J. Konigsberg, and T.M. Liss, FERMILAB-FN-0741 (2003).
[14] T. Sjostrand *et al.* , JHEP **0207**, 012 (2002).
[15] J. Pumplin *et al.* , Comput. Phys. Commun. **135**, 238 (2001).
[16] D. Acosta *et al.* (CDF Collaboration), Phys. Rev. Lett. **91**, 241904 (2003).
[17] A. Bhatti *et al.* , Nucl. Instrum. Methods A **566**, 375 (2006).
[18] F. Abe *et al.* (CDF Collaboration), Phys. Rev. D **45**, 1448 (1992).
[19] Particle Data Group, Phys. Lett. B **592**, 1 (2004).

TABLE IX: Background samples normalization

Sample	σ	N_{evt}^{gen}	Filter efficiency	L_{eff}	$f = L_{100}/L_{eff}$
$\mu + x$	$0.5091mb$	6238383	0.000239	$51.2709pb^{-1}$	1.9504
4 leptons	$0.538pb$	10995	1.0	$20436.803pb^{-1}$	0.0049
J/ψ	$0.127.2nb$	1413803	0.0074	$1502.00pb^{-1}$	0.0666

[20] P. Sutton, A. Martin, R. Roberts, and W. Stirling, Phys. Rev. D **45**, 2349 (1992); R. Rijken and W. van Neerven, Phys. Rev. D **51**, 44 (1995); R. Hamberg, W. van Neerven, and T. Matsuura, Nucl. Phys. B **359**, 343 (1991); R. Harlander and W. Kilgore, Phys. Rev. Lett. **88**, 201801 (2002); W. van Neerven and E. Zijstra, Nucl. Phys. B **382**, 11 (1992).
[21] A. Martin, R. Roberts, W. Stirling, and R. S. Thorne, Eur. Phys. J. C **28**, 455 (2003).
[22] R.Brun *et al.* , GEANT Detector Description and Simulation Tool, CERN Program Library, W5013, 1994.
[23] G. Abbiendi *et al.* (OPAL Collaboration), Eur. Phys. J. C **18**, 425-445 (2001).
[24] G. Abbiendi *et al.* (OPAL Collaboration), Eur. Phys. J. C **27**, 483-495 (2003), arXiv:0209068v1 [hep-ex].
[25] U. Ellwanger, J.F. Gunion and C. Hugoine, JHEP **0502**, 066 (2005).
[26] U. Ellwanger, C. Hugoine, Comput. Phys. Commun. **175**, 290 (2006).
[27] F. Domingo and U. Ellwanger, arXiv:0710.3714 [hep-ph].

VI. APPENDIX

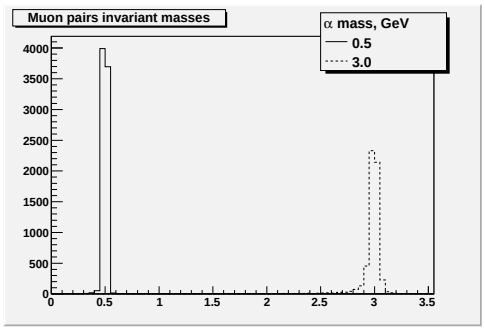

FIG. 5: Muon pairs invariant masses (m_H = 100 GeV)

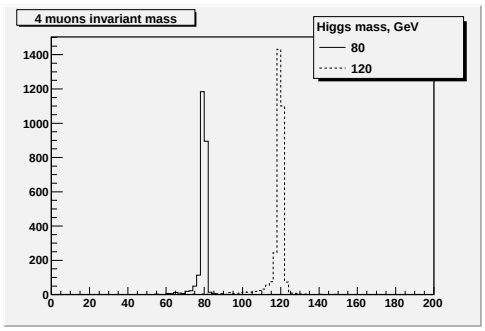

FIG. 6: 4 muons invariant mass (m_a = 3.0 GeV)

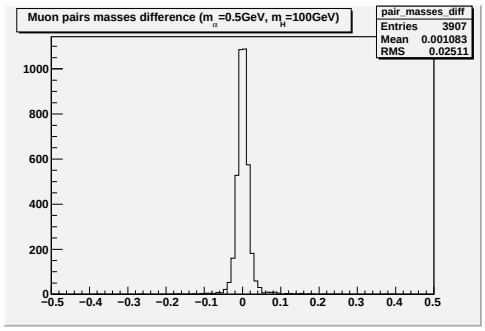

FIG. 7: Muon pairs masses difference (m_a=0.5GeV, m_H=100 GeV)

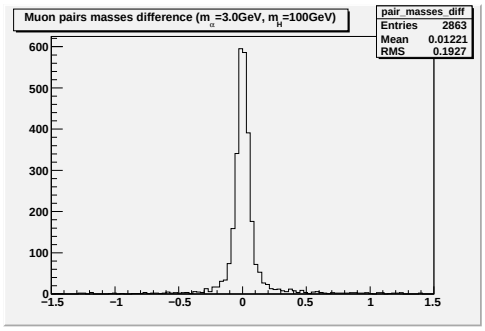

FIG. 8: Muon pairs masses difference (m_a=3.0GeV, m_H=100 GeV)

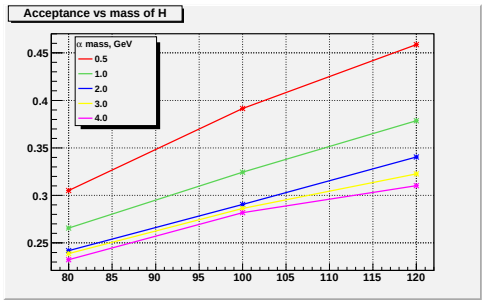

FIG. 9: Acceptance as a function of m_h for fixed m_a

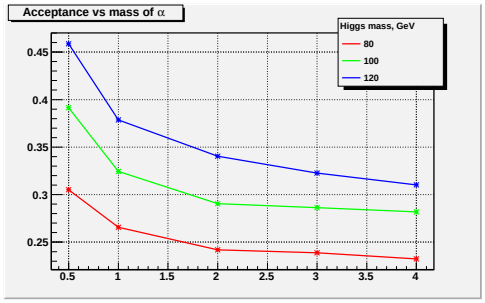

FIG. 10: Acceptance as a function of m_a for fixed m_h

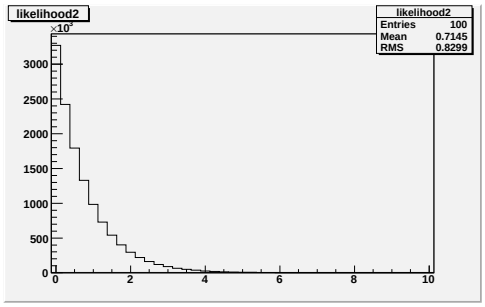

FIG. 11: Example likelihood for a pseudoexperiment for a search assuming $B(H{\to}aa{\to}\mu\mu\mu\mu)$=0.04, $m_a = 3$ GeV, $m_h = 100$ GeV with null signal shows that a 95% exclusion is somewhere around 2.5 pb for $\sigma(pp{\to}H)$.

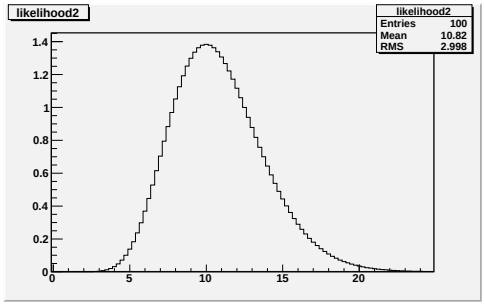

FIG. 12: Example likelihood for $\sigma(pp{\to}H)$=10 pb^{-1}, $B(H{\to}aa{\to}\mu\mu\mu\mu)$=0.04, $m_a = 3$ GeV $m_h = 100$ GeV shows a more than 5σ observation.